WIS-77/2-Ph

# Prompt γ-rays Emitted in Fission of $^{226}$Ra by 12 MeV Protons

A. Gayer and Z. Fraenkel

Weizmann Institute of Science

Rehovot, Israel

Abstract

The total energy associated with the emission of prompt γ-rays in fission of $^{226}$Ra induced by 12 MeV protons was measured in correlation with the fragment mass and kinetic energy. The dependence of the average total γ-ray energy on fragment mass and total kinetic energy resembles the corresponding dependence of the average number of neutrons. Using these results and the results for the average number of neutrons, we calculated the excitation energy of the fragments at the scission point. The results support the view that the scission-point configuration for the symmetric fission mode is more elongated than that for the asymmetric mode.

NUCLEAR REACTIONS, FISSION $^{226}$Ra(p,f), E = 12 MeV ; measured coin. fragment energy, γ-ray energy at 0° with respect to fragment; deduced total γ-ray energy emitted from the fission fragments.

## I. Introduction

The study of the total γ-ray energy emitted in fission, has been made so far only for nuclei which fission asymmetrically. Results for the spontaneous fission of $^{252}Cf$ and thermal neutron fission of $^{235}U$ and $^{239}Pu$ were reported by various authors[1-4]. The gross features of the γ-ray emission for these nuclei were summarized by Nifenecker et al.[5]. They appear to be in agreement with the predictions of a statistical deexcitation of the fission fragments, although the importance of the angular momentum effects for the deexcitation process is uncertain[2,4]. For all nuclei studied, the dependence of the total γ-ray energy on the fragment mass, resembles the corresponding dependence of the neutron multiplicity.

In the present experiment we have measured the total γ-ray energy emitted in the fission of $^{226}Ra$ by 12 MeV protons in correlation with the fragment mass and kinetic energy. The mass distribution was described by us in Ref. 6. It is triple-peaked, with almost equal contributions of the symmetric and asymmetric fission modes. It is therefore of interest to compare the present results with those obtained for asymmetric fission, and with the predictions for symmetric fission of the Liquid Drop Model.

Another purpose of the present experiment was to complete our information, obtained from the neutron measurement[6], regarding the excitation energy of the fission fragments. Using the known results for the total kinetic energy[6], and the excitation energy of the fragments, one can study the difference in the scission deformation between the symmetric and asymmetric modes.

In the present experiment, the γ-ray energy was measured by plastic scintillators placed at 0° to the fission axis. The discrimination between neutrons and gammas was obtained by measuring the time-of-flight to the scintillator.

The experimental technique and the method of data analysis are described in the next section. In Sec. III we present our results and discuss their significance.

## II. Experimental Method and Data Analysis

The experimental method was similar to that used by Nardi et al.[4] for measuring the total γ-ray energy in the spontaneous fission of $^{252}Cf$. The γ-ray energy was measured by a plastic scintillator (NE 102) placed at 0° to the fission axis, and the fragment energies were determined by a pair of solid-state detectors, placed on both sides of the $^{226}Ra$ target. In addition to the above three parameters, we also measured the time-of-flight to the scintillator, in order to distinguish between neutrons and gammas. The main advantages of this method are:

1) There is no need for an unfolding procedure of the γ-ray energy spectrum, because the energy absorption efficiency of the plastic scintillator is almost energy independent[7].
2) Good separation between gammas and neutrons is obtained by using plastic scintillators for the time-of-flight measurement. The width of the time-of-flight γ-peak was in our experiment 1.8 nsec FWHM, and it was almost completely separated from the neutron spectrum.

The experimental system was identical to that described in the preceding paper[6], except for the electronic system, which was modified to measure the energy absorbed in the scintillator. The linear signal from the photomultiplier was fed into two linear amplifiers which operated at different gains. The high-gain amplifier was adjusted to measure the energy spectrum in the 11-341 keV range, whereas the low-gain amplifier was adjusted to measure energies in the 0.341-5.0 MeV range. In this way each of the two photomultipliers measured the whole energy spectrum. The energy calibration was determined for each photomultiplier using the Compton edge of the following γ-ray sources: $^{203}Hg$, $^{22}Na$, $^{137}Cs$, $^{54}Mn$, $^{60}Co$. The energy absorption efficiency $\eta(E)$ is defined by the following equation:

$$\eta(E) = \int_{E_{min}}^{E} n(\varepsilon)\varepsilon \, d\varepsilon / N_o E \qquad (1)$$

where $N_o$ is the number of photons of energy E emitted by the γ-ray source, and $n(\varepsilon)$ the corresponding experimental spectrum. Using this equation $\eta(E)$ was derived for each γ-ray source, and the results are shown in Fig. 1 as a function of the photon energy. We see that $\eta(E)$ becomes almost flat at energies above 0.75 MeV, in agreement with the Monte Carlo calculations of Nardi[7]. At 0.6 MeV and 0.3 MeV $\eta(E)$ differs by 10% from the value at higher energies.

The data analysis was made using the method of Maier-Leibnitz et al.[8]. Using this method, the contribution of each fragment could be determined due to the asymmetry between 0° and 180° to the fragment direction, which is caused by the Doppler effect, and the change of the effective solid angle of the detectors. A detailed description of

this method is given in Refs. (4) and (8). The calibration method of Schmitt et al.[9] was used for the determination of the fragment masses and energies by an iteration procedure. This procedure and that for the time-of-flight calculation are summarized in the preceding publication[6].

## III. Results and Discussion

### A. Total γ-Ray Energy

Fig. 2 shows the average detected γ-ray energy per detected photon $\bar{\varepsilon}_\gamma(A_1,A_2)$, as a function of the fragment mass ratio. It is reasonable to assume that $\bar{\varepsilon}_\gamma(A_1,A_2)$ reproduces the trend of the average photon energy, emitted in fission, as a function of the mass ratio. We see that $\bar{\varepsilon}_\gamma$ reaches the highest value for the mass division 95,132 for which the heavy fragment is close to the doubly magic nucleus (50,82). A similar result was obtained for the spontaneous fission of $^{252}Cf$ by Nardi et al.[4], and can be explained by the lower level density of nuclei in the closed-shell region.

The total γ-ray energy released in a fission event, averaged over all mass-kinetic energy bins, was found to be $\bar{E}_{\gamma_T} = 6.02\pm0.50$ MeV/fission. This value is, within errors, equal to the corresponding values obtained for thermal-neutron fission of $^{235}U$ and $^{239}Pu$, and the spontaneous fission of $^{252}Cf$ [3,4] as shown in Table I.

The average total γ-ray energy emitted by a fragment $\bar{E}_\gamma(A,E_k)$, as a function of mass A and total kinetic energy $E_k$, was derived according to the method of Maier-Leibnitz et al.[8], for mass-kinetic energy bins of 4 amu width in the fragment mass and 4 MeV width in the total kinetic energy. The weighted average total γ-ray energy $\bar{E}_\gamma(A)$ as a function of

the fragment mass A, was obtained from $\bar{E}_\gamma(A,E_k)$ and is shown in Fig. 3. The structure of $\bar{E}_\gamma(A)$ is very similar in shape to that of the average number of neutrons $\bar{\nu}_a(A)$, previously presented in Ref. 6. We see that $\bar{E}_\gamma(A)$ is also a combination of a "saw-tooth" structure in the asymmetric mass division region, and a monotonically increasing function in the symmetric region. The similarity in the structure of $\bar{E}_\gamma(A)$ and $\bar{\nu}_a(A)$ was already observed for the thermal neutron fission of $^{235}U$ [1] and the spontaneous fission of $^{252}Cf$ [4]. According to Nardi et al.[4] this behaviour can be explained chiefly by the correlation between the average number of neutrons, and the neutron binding energy of the residual nucleus.

The average total γ-ray energy $\bar{E}_{\gamma_T}(E_k)$ emitted in fission, as a function of the kinetic energy of the two fragments, was obtained by a weighted average of $\bar{E}_\gamma(A,E_k)$ and is shown in Fig. 4. We see that over most of the kinetic-energy distribution, $\bar{E}_{\gamma_T}(E_k)$ decreases linearly with increasing $E_k$, similar to the variation of $\bar{\nu}_a(E_k)$ [6]. The average derivative of $\bar{E}_{\gamma_T}$ with respect to $E_k$, $\left\langle \frac{\partial \bar{E}_{\gamma_T}}{\partial E_k} \right\rangle$ (averaged over A and $E_k$) is 0.035±0.005, in agreement with the result of Nardi et al.[4] for $^{252}Cf$. This supports the conclusion of Nardi et al.[4], that the variation of $\bar{E}_\gamma(A,E_k)$ is explained chiefly by the variation of the neutron binding energy.

B. Excitation Energy

The results for the total γ-ray energy of the present experiment complement our measurement of the prompt neutrons[6], in that it is possible to obtain from the combined measurement the excitation energies of the fission fragments. The final excitation energy of the fragment

$\bar{E}_x$ is obtained by the equation:

$$\bar{E}_x = \bar{\nu}_a(\overline{BE} + \bar{\eta}_a) + \bar{E}_\gamma \qquad (2)$$

where $\overline{BE}$ and $\bar{\eta}_a$ are the average neutron binding energy and kinetic energy respectively. The average neutron binding energy $\overline{BE}(A)$ was calculated using the mass tables of Garvey et al.[11]. For every mass bin A, $\overline{BE}$ was obtained by a weighted average of the binding energies of all fragments corresponding to that bin. A gaussian charge distribution with a width of 0.7 charge units[12] was taken as a weighting function. The most probable charge for a given fragment mass was obtained based on the assumption of unchanged charge-to-mass ratio[12] (the average binding energy was insensitive to this assumption). The average binding energy $\overline{BE}(A)$, as a function of the fragment mass is shown in Fig. 5. Using this procedure, we obtained the average excitation energy $\bar{E}_x(A)$, which is shown in Fig. 6 as a function of the fragment mass A. As expected, the structure of $\bar{E}_x(A)$ resembles that of $\bar{\nu}_a(A)$ and $\bar{E}_\gamma(A)$. The behavior of $\bar{E}_x(A)$ for the symmetric and asymmetric modes was obtained by a parabolic cut in the mass-energy plane as discussed in Ref. 6, and is shown in Fig. 7 together with the corresponding mass distributions. We see that for the symmetric mode, the excitation energy increases almost linearly with the fragment mass (except for the small dip at mass ~103 which is due to a small contribution of asymmetric mode), in qualitative agreement with the LDM calculation of Nix and Swiatecki[13]. But the experimental slope $\frac{d\bar{E}_x}{dA}$ is 0.63±0.05 MeV/amu as compared to 0.16 MeV/amu predicted by the LDM calculation. Our result is close to the result of Plasil et al.[14], who obtained

0.78±0.03 MeV/amu for the fission of $^{213}$At. For the asymmetric mode, $\bar{E}_x(A)$ has a "saw-tooth" structure as is generally obtained for asymmetric fission.

The average total excitation energy for the two modes, together with the corresponding average total kinetic energies are summarized in Table II. We see that although the total energy released in the fission process $\bar{E}_T$, is almost equal for the two modes (this is confirmed by a calculation using the mass tables of Ref. 11), the excitation- and kinetic energies are quite different for the two modes. This result may be explained by a somewhat different scission configurations for the two modes. The higher excitation energy and lower kinetic energy for the symmetric fission mode, are consistent with a more elongated scission configuration compared to the asymmetric fission configuration.

In order to get a more quantitative picture of the difference between the two scission configurations, we used a simplified version of the Liquid Drop Model. The nucleus at the scission point was described by two almost touching coaxial spheroids. The configuration was specified by the following four parameters: the distance $\ell$ between the centers of the two spheroids, the fractional mass U of one fragment and the major axes $c_1$, $c_2$ of the two spheroids (see Fig. 8). The major axes $c_1$, $c_2$ for each fission mode were calculated from the experimental values of the deformation energies of the two fragments, using the formula derived by Nix and Swiatecki[13]. The deformation energy was obtained from our results for the excitation energy, by subtracting a relative part of the excitation energy of the nucleus at the saddle point, according to the average fragment mass in each fission

mode. Using the calculated values of $c_1, c_2$ and the experimental values of the total kinetic energy we could calculate the distance $\ell$ between the centers of the spheroids. This was done according to the formula for the Coulomb interaction energy derived in Ref. 13, and assuming the pre-scission kinetic energy to be zero. Table III summarizes the results for the major axes and the distance between the centers, together with experimental values of the excitation and deformation energies. We see that the deformation of the fragments, as characterized by the ratio of the major axis to the radius of a spherical drop of the same volume, is higher by about 20% for the symmetric mode as compared to the asymmetric mode.

Table I. The average total γ-ray energy $\bar{E}_{\gamma_T}$ per fission, for various fissionning nuclei.

| Type of Fission | $\bar{E}_{\gamma_T}$ (MeV) |
|---|---|
| $^{226}Ra$ + 12 MeV p | 6.02 ± 0.50 |
| $^{235}U$ + n | 6.51 ± 0.30[a] |
| $^{239}Pu$ + n | 6.82 ± 0.30[a] |
| $^{252}Cf$ S.F. | 6.84 ± 0.30[a] |

(a) Ref. 3.

Table II. The average total γ-ray energy $\bar{E}_{\gamma_T}$, the average total kinetic energy $\bar{E}_K$, the average excitation energy $\bar{E}_{x_T}$ and the total energy $\bar{E}_T$ released in the fission process of $^{227}Ac$ for the symmetric and asymmetric modes separately, and for both modes combined.

| | Both Modes | Symmetric Mode | Asymmetric Mode |
|---|---|---|---|
| $\bar{E}_{\gamma_T}$ (MeV/fission) | 6.02 ± 0.50 | 6.64 ± 0.60 | 5.42 ± 0.50 |
| $\bar{E}_K$ (MeV/fission) | 155.9 ± 2.0 | 151.7 ± 2.0 | 160.0 ± 2.0 |
| $\bar{E}_{x_T}$ (MeV/fission) | 28.6 ± 1.6 | 33.3 ± 1.9 | 23.1 ± 1.2 |
| $\bar{E}_T$ (MeV/fission) | 184.5 ± 3.6 | 185.0 ± 3.9 | 183.1 ± 3.2 |

Table III. The average excitation energy $\bar{E}_x$ and deformation energy $\bar{E}_{def}$ for the light and heavy fragment, the calculated major axes c of the fragments, the distance $\ell$ between the centers and the distance d between the tips of the two spheroids, for the symmetric and asymmetric modes. R is the radius of a spherical drop of the same volume as the corresponding fragment.

| | Symmetric Mode | Asymmetric Mode | |
|---|---|---|---|
| | single fragment | light fragment | heavy fragment |
| $\bar{E}_x$ (MeV) | 16.6 | 10.6 | 12.5 |
| $\bar{E}_{def}$ (MeV) | 12.2 | 6.7 | 6.4 |
| c (fermi) | 10.2 | 8.5 | 9.6 |
| c/R | 1.73 | 1.56 | 1.54 |
| $\ell$ (fermi) | 20.6 | 18.5 | |
| d (fermi) | 0.2 | 0.4 | |

## References


1) F. Pleasonton, R.L. Ferguson and H.W. Schmitt, Phys. Rev. C 6, 1023 (1972).

2) H. Nifenecker, C. Signarbieux, M. Ribrag, J. Poitou and J. Matuszek, Nucl. Phys. A189, 285 (1972).

3) V.V. Verbinski, H. Weber and R.E. Sund, Phys. Rev. C 7, 1173 (1973).

4) E. Nardi, A. Gavron and Z. Fraenkel, Phys. Rev. C 8, 2293 (1973).

5) H. Nifenecker, C. Signarbieux, R. Babinet and J. Poitou, in Proceedings of the Symposium on the Physics and Chemistry of Fission, Rochester, 1973 (IAEA, Vienna 1974), Vol. II, p. 117.

6) A. Gayer and Z. Fraenkel (preceding paper).

7) E. Nardi, Nucl. Instrum. Meth. 95, 229 (1971).

8) H. Maier-Leibnitz, H.W. Schmitt and P. Armbruster, in Proceedings of the Symposium on the Physics and Chemistry of Fission, Salzburg, 1965 (IAEA, Vienna 1966), Vol. 2, p. 143.

9) H.W. Schmitt, W.E. Kiker and C.W. Williams, Phys. Rev. 137, B837 (1965).

10) G. Mehta, J. Poitou, M. Ribrag, C. Signarbieux, Phys. Rev. C 7, 373 (1973).

11) G.T. Garvey, W.J. Gerace, R.L. Jaffe, I. Talmi and I. Kelson, Rev. Mod. Phys. 41, 51 (1969).

12) R. Vandenbosch, J.R. Huizenga, Nuclear Fission (Academic Press 1973) p. 324.

13) J.R. Nix, W.J. Swiatecki, Nucl. Phys. 71, 1 (1965).

14) F. Plasil, R.L. Ferguson, H.W. Schmitt, in Proceedings of the Second Symposium on the Physics and Chemistry of Fission, Vienna, 1969 (IAEA, Vienna, 1969) p. 505.

## Figure Captions

Fig. 1. The energy absorption efficiency $\bar{\eta}(E)$ as a function of the γ-ray energy, normalized to 1.0 at 0.662 MeV.

Fig. 2. The average detected γ-ray energy per detected photon $\bar{\varepsilon}_\gamma(A_1,A_2)$ as a function of the fragment mass ratio. The statistical errors can be inferred from the fluctuations between neighboring points.

Fig. 3. The average total γ-ray energy $\bar{E}_\gamma(A)$ as a function of the fragment mass A. The mass distribution Y(A) is shown by a dashed curve for reference. Where the statistical errors are not given, they are too small to be shown.

Fig. 4. The average total γ-ray energy $\bar{E}_{\gamma_T}(E_k)$ as a function of the kinetic energy of the two fragments $E_k$. The kinetic energy distribution $Y(E_k)$ is shown by a dashed line for reference. Where the statistical errors are not given, they are too small to be shown.

Fig. 5. The average neutron binding energy $\overline{BE}$ as a function of the fragment mass A. $\overline{BE}$ was derived from the mass tables of Garvey *et al.*[11]

Fig. 6. The average excitation energy $\bar{E}_x(A)$ as a function of the fragment mass A. The mass distribution Y(A) is shown by a dashed line in arbitrary units, for reference. The statistical errors are too small to be shown.

Fig. 7. The average excitation energy $\bar{E}_x(A)$ as a function of the fragment mass A, for the symmetric mode and the asymmetric mode. The corresponding mass distributions Y(A) are shown

Fig. 7. (cont'd) by dashed lines. The statistical errors are too small to be shown.

Fig. 8. Schematic representation of the model used in the calculation.

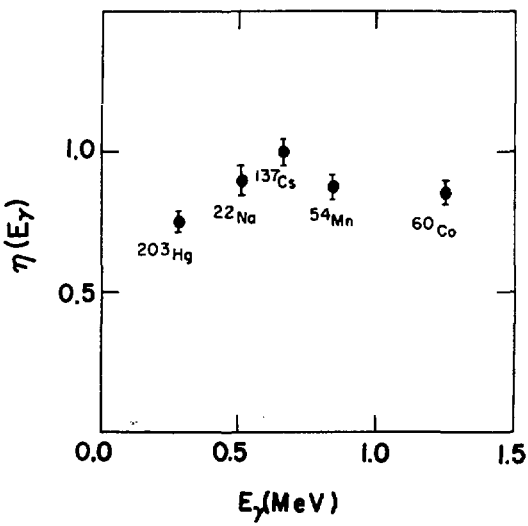


Fig. 1

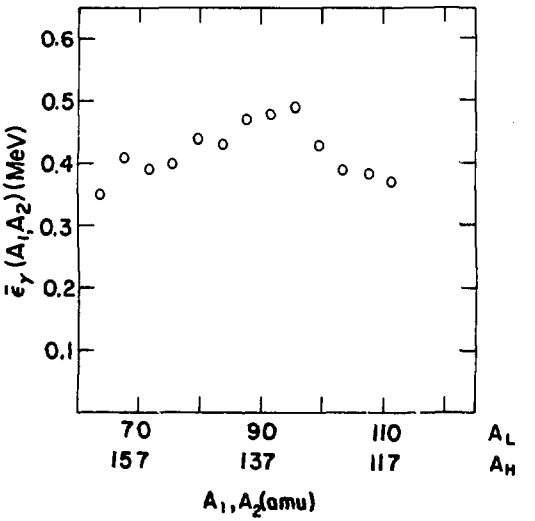
0.6
0.5
0.4
0.3
0.2
0.1
$\bar{\epsilon}_\gamma(A_1,A_2)$(MeV)
70
157
90
137
110
117
$A_L$
$A_H$
$A_1, A_2$(amu)

Fig. 2

1P

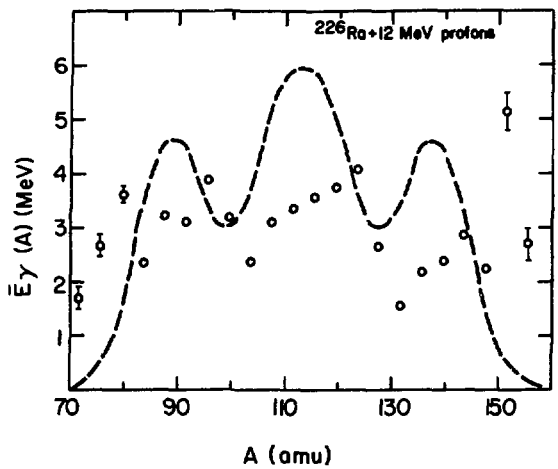


Fig. 5

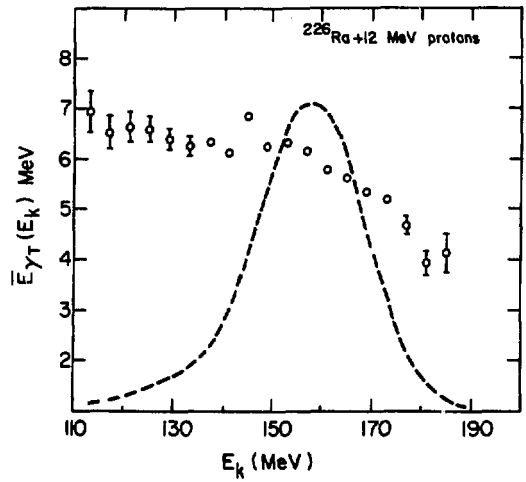
226Ra+12 MeV protons
$\bar{E}_{\gamma T}(E_k)$ MeV
$E_k$ (MeV)
2
3
4
5
6
7
8
110
130
150
170
190

Fig. 3

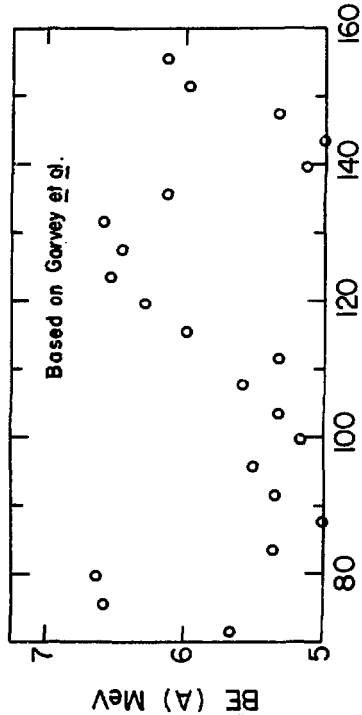


Fig. 5

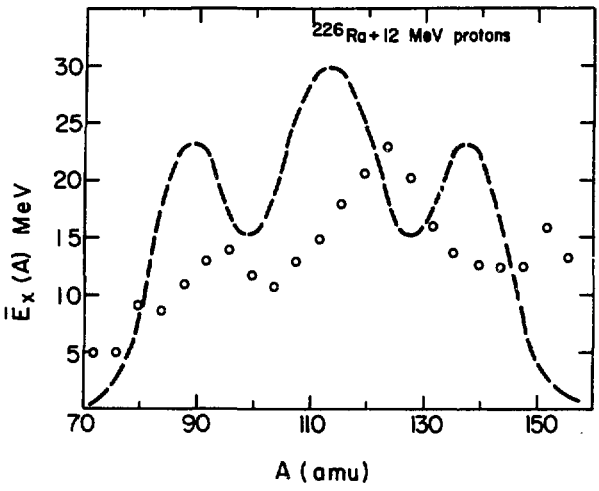
$^{226}$Ra+12 MeV protons
$\bar{E}_x$ (A) MeV
30
25
20
15
10
5
70
90
110
130
150
A (amu)

Fig. 6

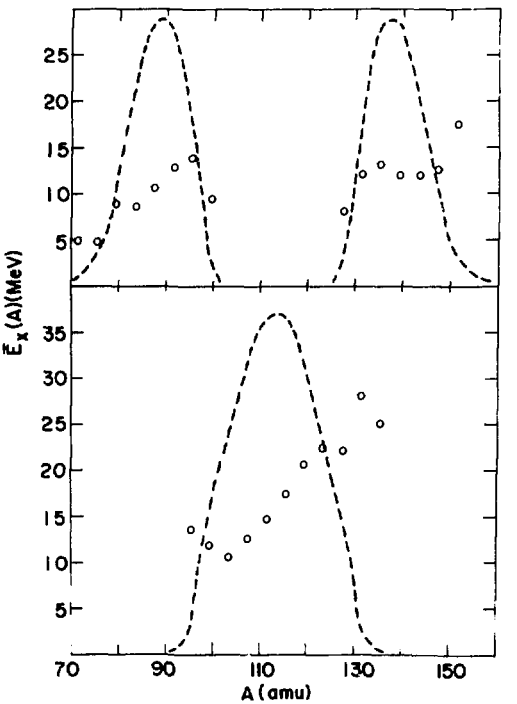


Fig. 7

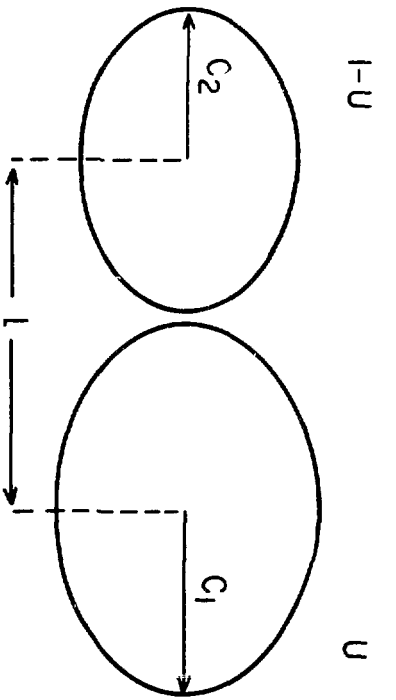


fig. 8